Combustion Analysis of Ammonia/Oxygen Mixtures at Various Equivalence Ratio Conditions Using a Constant Volume Combustor with Sub-chamber

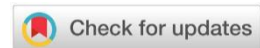**Bin Guo[1], Mitsuhisa Ichiyanagi[2], Makoto Horie[1], Keita Aihara[1], Takuma Ohashi[2], Abiyasu Zhang[2], Takashi Suzuki[2]✉**

[1]Graduate School of Science and Technology, Sophia University, Tokyo, 102-8554, Japan
[2]Department of Engineering and Applied Sciences, Sophia University, Tokyo, 102-8554, Japan

✉ suzu-tak@sophia.ac.jp

Check for updates

Abstract

The greenhouse effect issue is becoming more serious, and renewable energy is playing an increasingly important role. Among all alternative fuels, ammonia has been attracting attention as a carbon-free energy carrier for hydrogen, because of its large energy density per volume and easy storage and transportation. On the other hand, ammonia has a low combustion speed, which is an important issue for the use of ammonia as a vehicle fuel. To increase the mean flame speed of ammonia, the present study used the burned gas ejected from the sub-chamber for the compression of the mixture in the main chamber and the promotion of its HCCI combustion. Thus, the constant volume combustor with sub-chamber was used to realize the above combustion and to study the combustion characteristics of ammonia and oxygen mixture. In the experiments, initial pressure and initial temperature were unchanged and only the equivalence ratio was changed. The combustion pressure data were recorded and analyzed. As the result, the maximum combustion pressure (2.5 MPa) was obtained when the equivalence ratio was 0.4. The combustion speed was the fastest when the equivalence ratio was 0.6, and the mean flame speed was about 57.5 m/s.

Keywords: Spark ignition engine; Alternative fuel, Ammonia, Constant volume combustor

1. Introduction

Renewable energy is playing an increasingly important role in addressing some of the key challenges facing today's global society, such as the cost of energy, energy security and climate change. The exploration of renewable energy looks set only to increase across the globe as nations seek to meet their legislative and environmental obligations with respect to greenhouse gas emissions [1]. In Japan, greenhouse gas emissions were 1.138 billion tons of CO_2 as of year 2018, of which CO_2 emissions from the transportation sector, including automobiles, trains, buses, and ships, accounted for 210 million tons, or about 18.5% of overall. Passenger cars and freight cars emit 49.6% and 36.6% of the total transport sector, respectively. The reduction of carbon dioxide emissions in the automobile industry is essential, and there is an urgent need to improve the fuel efficiency of internal combustion engines, which are the main source of power for automobiles. In addition, the emission regulations of automobiles in various countries are becoming stronger year by year, and this trend is expected to continue in the future [2].

Some previous studies have produced more sustainable fuels with low to zero net carbon emissions as alternative energy sources [3][4] to reduce the damage of fossil fuels. The alternative fuels include biofuel [5][6], hydrogen [7], and ammonia [8]. Among them, because the product of hydrogen combustion is only water, it is not harmful to the environment at all, and this is the

most eye-catching. But the current difficulty in the utilization of hydrogen energy is mainly the storage and transportation of hydrogen. As shown by data, at atmospheric pressure, hydrogen can be liquefied only when the temperature is lower than 20 K [9]. To maintain such a low temperature to transport liquid and store hydrogen will inevitably lead to high costs. For the above reasons, ammonia has been attracting attention as a carbon-free energy carrier for hydrogen. Compared with hydrogen, at atmospheric pressure, ammonia can be liquefied only by lowering the temperature to 240 K. In addition, the energy density of liquid hydrogen is 8.5 MJ/*l*, and the energy density of liquid ammonia is 12.7 MJ/*l* [9]. As can be seen from the above, the cost of ammonia in storage and transportation is relatively small. In addition, as an important industrial raw material, ammonia has been used for nearly 100 years, which means that ammonia production technology is more mature and production costs are lower. Ashida et al. researched a highly active catalyst for the synthesis of ammonia under normal temperature and pressure conditions [10]. Therefore, it can be expected that the production cost and production energy consumption of ammonia will be lower in the future.

Based on the above advantages, many researchers have studied the combustion and utilization of ammonia and related issues. Saika et al. studied hydrogen supply system with ammonia, which worked under the condition of catalyst temperature 800°C, the pressure of 100 kPa [11]. Xia et al. studied coal/ammonia co-combustion, which clarified the mechanism of difference of the flame propagation velocities between co-combustion and pure ammonia combustion under different ammonia content conditions [12][13]. Takeishi et al. used the burner to study ammonia/N_2/O_2 laminar flame in oxygen-enriched air condition, which showed when the oxygen concentration 35%, the equivalence ratio 1.1, the ammonia laminar burning velocity can reach 36.1 cm/s [14]. Ito et al. tested ammonia/natural gas co-firing power generation gas turbine, which showed 20%LHV ammonia can be completely combusted and reduced the CO_2 emission compare with nature gas turbine [15]. Those studies show a huge potential for ammonia used as fuel for generating electricity.

Gross and Kong studied direct-injection ammonia–DME mixtures used in CI engine, which showed the inclusion of ammonia in the fuel mixture can reduce the soot emission, but may result in higher CO and HC emissions [16]. And by increasing in injection pressure, ammonia content could be higher and lead to improved combustion and emissions. Frigo and Gentili studied stoichiometry ammonia/hydrogen mixture performance in a spark-ignition (SI) engine, which showed engine stability increases with increasing the hydrogen-to-ammonia energy ratio [17]. Pochet et al. studied ammonia/hydrogen mixture performance in HCCI engine, which provided a direction of decrease NOx emission produced by burning ammonia, by using EGR [18]. Since most studies tend to use ammonia as the fuel for power plants or combine ammonia with other fuels, the problem of low combustibility of ammonia is easily to be neglected. This makes it difficult for ammonia to be used as a fuel for IC engines, because internal combustion engines have very high requirements for fuel combustion speed. Some studies showed that the jet from the sub-chamber was proved to promote combustion [19]-[21]. Additionally, multi-stage combustion was proved to be effective in promoting combustion [22][23]. However, to our knowledge, detailed characteristics for ammonia combustion have not been investigated when combining with sub-chamber and multi-stage combustion.

The purpose of the present study is to increase the mean flame speed of ammonia to reach the level of hydrocarbon fuel, so as to achieve the goal of using ammonia as IC engine fuel. Therefore, we conducted the combustion experiment of ammonia and oxygen mixture using the constant volume combustor with a sub-chamber under various equivalence ratio conditions, and clarified the combustion characteristics of ammonia under this condition.

2. Experiment Apparatus and Experimental Procedure

2.1. Experiment apparatus

Figure 1 shows the cross-sectional schematic diagram of the constant volume burner used in the experiment. The cylinder head used in the constant volume combustor is based on the Yammer TF120V-E diesel engine. We machined

the hole of the original injector, and installed the spark plug (NGK-CR8E) on the cylinder head through an adapter in the sub-chamber. The pressure sensor (Kistler 6054 BR-3-1) was installed on the top of the main chamber. Install the cylinder head on the base plate to form the constant volume combustor used in the experiment. The yellow part in **Figure 1** constitutes the lower surface of the main chamber. The shape of this part is simplified from the plane piston (diameter: 92mm). The overall volume of the combustor is about 42.5cc, including a 23.5cc sub-chamber and a 19cc main chamber. The main chamber and sub-chamber are connected by an orifice with a cross-sectional area of 52.6 mm². The purpose of using a constant volume combustor of this structure is to keep it as consistent as possible with the actual engine combustor structure.
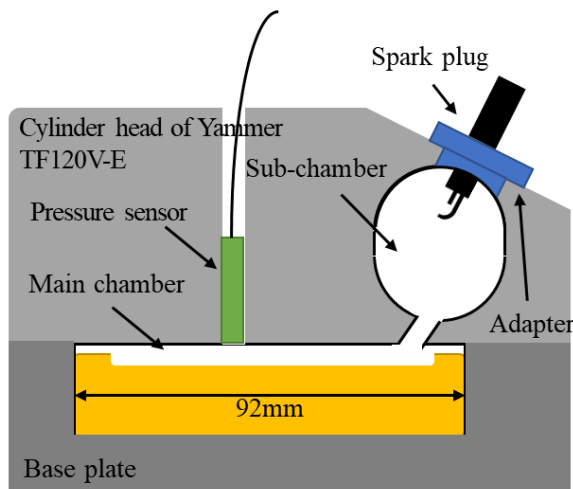

Figure 1. Schematic of the constant volume combustor

A schematic diagram of the experimental apparatus is shown in **Figure 2**. In the upstream position of constant volume combustor are ammonia cylinder and oxygen cylinder. A pressure gauge (NAGANO GC04) is installed on the pipe connecting the constant volume volume combustor and cylinders to monitor the pressure in the pipe (pressure in the constant volume combustor). In the downstream position of the constant volume combustor are the catalyst (used to purify the exhaust after combustion), the cooling pipe (to protect the vacuum pump), the vacuum pump, and the gas washing bottle with activated carbon. On the outlet side of the vacuum pump, there is a pipe connected to the upstream of the catalyst. The purpose is to circulate the exhaust gas through the catalyst through the

vacuum pump to achieve sufficient purification. The pressure change caused by the combustion of the mixture is measured by the pressure sensor installed in the main chamber, and then transferred to the data logger (RIGOL DS 1202Z).
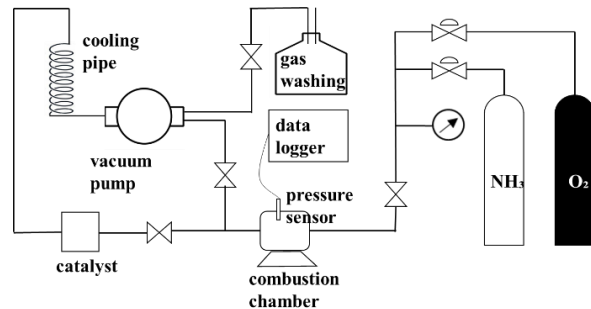

Figure 2. Schematic diagram of the experimental apparatus

2.2. *Experimental procedure*

The oxidation catalyst was heated to operational temperature, and oxygen was introduced into the pipeline to exhaust air or exhaust gas generated after combustion. Then a vacuum (absolute pressure 0.05 MPa) in the constant volume combustor was created by using a vacuum pump. Ammonia and oxygen were filled into the constant volume combustor. The spark plug was ignited in the sub-chamber and the in-cylinder pressure data was recorded. Finally, the combustion gas was circulated in the oxidation catalyst, sufficiently decomposed, and exhausted to the outside air.

3. Experiment Conditions and Analysis Methods

3.1. *Experimental conditions*

The experimental condition is shown in **Table 1**. In this experiment, the equivalence ratio was varied in the range of 0.1 to 1.4, and the partial pressures of ammonia and oxygen were varied according to the overall reaction equation. Pressure in the present study expresses by absolute pressure. Initial pressure was fixed at 0.2 MPa and initial temperature condition is the room temperature 298 K.

Table 1. Experimental condition

Initial Pressure [MPa]	0.2
Initial Temperature [K]	298
Equivalence Ratio [-]	0.1, 0.2~1.4
	(in 0.2 steps)

The equivalence ratio and the corresponding partial pressure of ammonia and oxygen are shown in **Table 2**, including the condition of incombustible (0.1, 1.4) and the condition of unstable combustion (1.2). Oxygen is used to exhaust the exhaust gas in the experimental device before each set of experiments, and then, the vacuum operation is performed. The vacuum cannot reach an absolute pressure of 0 MPa, but the vacuum operation can reach the absolute pressure of 0.05 MPa. Therefore, the sum of the partial pressures of ammonia and oxygen in **Table 2** is an absolute pressure of 0.15 MPa, which reachs total pressure 0.2 MPa of absolute pressure.

Table 2. Filling pressure (absolute pressure) of ammonia and oxygen

Equivalence ratio [-]	Ammonia pressure [MPa]	Oxygen pressure [MPa]
0.1	0.0235	0.129
0.2	0.0421	0.111
0.4	0.0696	0.083
0.6	0.0889	0.064
0.8	0.1032	0.050
1.0	0.1143	0.039
1.2	0.1231	0.030
1.4	0.1302	0.023

3.2. Analysis methods

3.2.1. Heat release rate

When combustion occurs, the pressure of the main combustor is measured by a pressure sensor attached to the cylinder head. The measured combustion pressure is then used to calculate the heat release rate. For constant volume combustor, the heat release rate is the amount of heat per unit time generated by combustion. And because of the combustion in the constant volume ombustion chamber, the gas volume will not change during the process. Therefore, the heat release rate can be expressed by the following Eq.(1).

$$\frac{dQ}{dt} = \frac{1}{\kappa - 1} \cdot V \frac{dP}{dt} \tag{1}$$

where $\frac{dQ}{dt}$: heat release rate [J/ms], P: combustion pressure [MPa], V: combustor volume [m³], t: time [ms], κ: specific heat ratio [-].

3.2.2. Percentage burned

Percentage burn η indicates the amount of fuel burned in an experiment relative to the amount of fuel that was inputted. Total heat released Q_{burned}

in the combustion can be calculated integrating the positive values of heat release rate in an experiment as Eq.(2).

$$Q_{burned} = \int \frac{dQ}{dt} \tag{2}$$

Fuel supplied to the constant volume chamber in n moles can then be converted to joules of heat as Q_{input} using Eq.(3).

$$Q_{input} = \frac{PV}{RT} * M_{NH3} * LHV_{NH3} \tag{3}$$

where R: Gas Constant [Pa*m³/(K*mol)], and T: initial temperature [K], M_{NH3}: molar mass of ammonia 17.031 [g/mol], LHV_{NH3}: lower heating value of ammonia 18.6 [MJ/kg]. Finally, percentage burned η relative to amount supplied can be calculated from Eq.(4).

$$\eta = \frac{Q_{burned}}{Q_{input}} * 100\% \tag{4}$$

3.2.3. Mean flame speed

In the present study, the mean flame speed $\bar{v}$ was obtained by dividing the combustion chamber diameter by the combustion time as Eq.(5).

$$\bar{v} = \frac{D}{t_c} \tag{5}$$

where D: piston diameter is 0.092 [m] and t_c: combustion duration defined as the time from heat release becoming positive to reaching zero.

3.2.4. Mass fraction burned and volume fraction burned

Mass fraction burned is the amount of fuel in terms of mass that was burned during the combustion relative to 100% burned. In the present study, the effect of heat loss was neglected, and the time at maximum combustion pressure was taken as the time of combustion completion, and the mass fraction burned r_m was calculated using Eq.(6).

$$r_m = \frac{m_b}{m} = \frac{(p - p_1)}{(p_2 - p_1)} \tag{6}$$

where m_b: the mass of burned gas [kg], m: the mass of gas before combustion [kg] p: the current pressure [MPa], p_1: the initial pressure [MPa], p_2: the maximum pressure [MPa].

For constant volume combustor, the volume fraction burned is defined as the volume of combustion gas divided by the total volume. Assuming that the unburned gas is adiabatically compressed by bured gas, the volume fraction burned r_v was calculated by Eq.(7).

$$r_v = \frac{v_b}{v} = \left[1 - \frac{1 - r_m}{[1 + r_m(\frac{p_2}{p_1} - 1)]^{1/\kappa}} \right] \quad (7)$$

where v_b: the volume of burned gas [m³], v: the volume of constant volume combustor [m³].

4. Result and Discussion

4.1. Combustion process

Figure 3 shows in-cylinder pressure and heat release rate at equivalence ratio 0.4 at 298 K. From the ignition timing at time 0, a linear increase in the in-cylinder pressure is recorded. And it can be seen that the heat release rate curve rises slowly at this time. After certain time after ignition, a rapid increase in pressure was measured at the time of 4.2ms, and reach the pressure peak in a short period of time. In the phase of rapid pressure rise, the corresponding heat release rate curve also rises sharply.
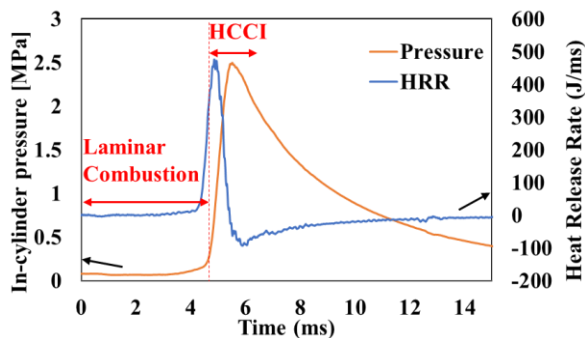

Figure 3. In-cylinder pressure (absolute pressure) and heat release rate at equivalence ratio 0.4

The linear increase in pressure representing the laminar flame combustion and the exponential increase in pressure is a typical tendency seen in homogeneous charge compression ignition. Due to the existence of the sub-chamber, unburned gas was ejected from the sub-chamber by expanded burned gas, compressing the unburned gas in the main combustor. Combustion in the sub-chamber was almost laminar burning speed because of without gas turbulence, and then compressed and turbulent unburned gas in the main-chamber was rapidly burned as HCCI combustion.

4.2. Effect of equivalence ratio

4.2.1. In-cylinder pressure (absolute pressure)

Experiment was conducted to observe the effect of different equivalence ratio to the combustion. **Figure 4** shows the measured in-cylinder pressure with different equivalence ratio at room temperature 298 K with initial pressure 0.1 MPa condition. Each equivalence ratio condition was conducted 5 times to acquire the average to reduce experimental errors and to smooth the data. During the experiments, the ammonia could be stable combusted under the condition of equivalence ratio 0.2 ~ 1.0. And under the condition of equivalence ratio 1.2, combustion did not happen for some experiment, thus, this condition is considered to be unstable combustion. Under the condition of equivalence ratio of 0.1 and 1.4, the mixture could not burn. Thus, the results only discuss the condition of equivalence ratio 0.2 to 1.0. As explained before, the experiment showcased that ammonia can be burned at relatively low lean condition of equivalence ratio 0.2, however it struggles to burn at rich conditions. The slope of the in-cylinder pressure differs for different equivalence ratio condition means the burning speed was different with each condition. It can be seen from the figure that when the equivalence ratio is 0.2 and 1.0, the peak combustion pressure is obviously lower. When the equivalence ratio is 0.2, the amount of ammonia used as fuel is small, resulting in a low combustion pressure. Since the maximum combustion pressure decreased even when the equivalence ratio was 1, it can be considered that the combustion efficiency is better when the oxygen concentration is larger [24].
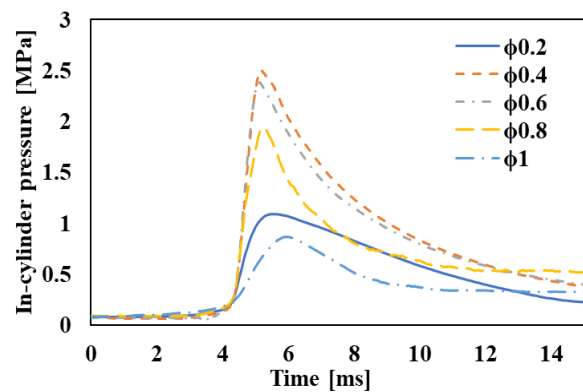

Figure 4. Measured in-cylinder pressure with different equivalence ratio at 298 K

Figure 5 shows the maximum in-cylinder pressure with different equivalence ratio. Average of 5 data is plotted in the graph as a connecting dot, and the vertical line shows the range of highest to lowest peak pressure value within the same equivalence ratio. From the figure, it can be seen that as the equivalence ratio decreases, the amount of oxygen to fuel increases, and thus the maximum combustion pressure increases. At the equivalence ratio of 0.2, the maximum pressure decreased due to unstable combustion near the combustion limit.
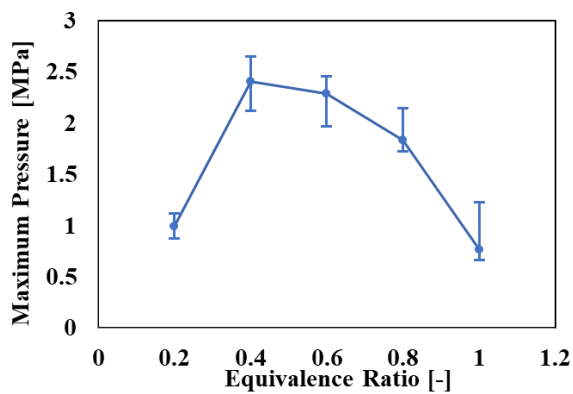

Figure 5. Maximum in-cylinder pressure with different equivalence ratio at 298 K

4.2.2. Percentage burned

Figure 6 is the percentage burned (the ratio of actual quantity of ammonia burned and ammonia supply quantity) with a different equivalence ratio at 298K calculated from equation 4. Equivalence ratio 0.4 had the highest percentage burned ratio of 87% and stoichiometry had the lowest of 17%.
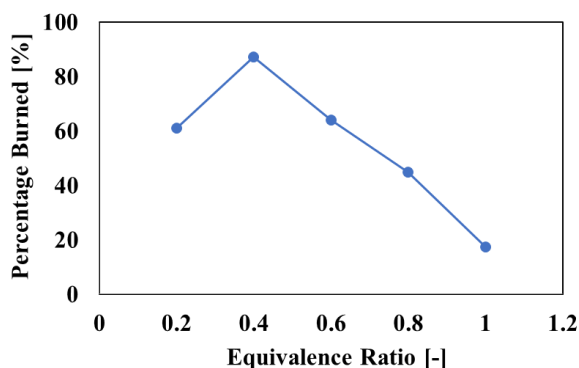

Figure 6. Percentage burned with different equivalence ratio at 298 K

At stoichiometry, 83% of ammonia fuel is being unburned. The result indicates that as the ammonia concentration increases, the percentage burned massively decreases, as following the tendency of maximum in-cylinder pressure as in

Figure 5. When the equivalence ratio is 0.2, the combustion percentage is also lower than the combustion percentage when the equivalence ratio is 0.4, which is 61%, which means that a too lean mixture will also cause insufficient combustion.

4.2.3. Mass fraction burned and volume fraction burned

Figure 7 represents the volume fraction burned (the ratio of the volume of burned gas at any time and the volume of constant volume combustor) versus the mass fraction burned (the ratio of the mass of burned gas at any time and actual quantity of ammonia burned) at different equivalence ratio calculated using equation 6 and 7. Mass fraction burned in the figure represents the percentage burned ammonia in relative to 100% burned, which differs from the percentage burned in **Figure 6** representing the percentage burned in terms of input ammonia. Sub-chamber volume is 23.5cc and main chamber volume is 19cc. The vertical line at 55% volume fraction burned represents the borderline between the volume of sub-chamber and the main chamber volume.
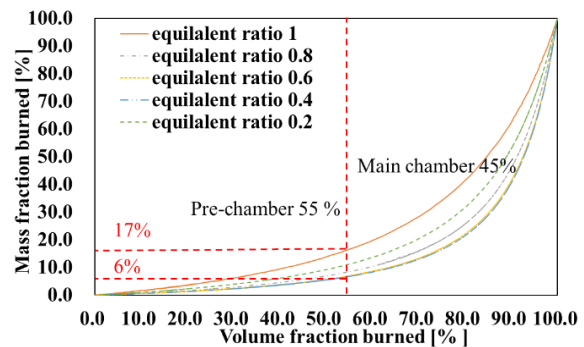

Figure 7. Mass fraction burned versus volume fraction burned at different equivalence ratio at 298 K

The graph of the relationship between the volume burned and mass burned can indicate where combustion occurs during the experiment. As shown in **Figure 7**, the curves of the relationship between the volume burned under each equivalence ratio are all exponential case. This shows that in the initial stage of combustion, the volume of burned gas expands rapidly, but the mass of the fuel actually burned is very small. Since the combustion occurs in the constant volume chamber, the total space remains constant. Under the expantion of the burned gas, the volume of the unburned gas decreases and the

temperature rises, leading to rapid combustion. As shown in the interval with a larger slope in the second half of the curve. At the borderline between the sub-chamber volume and main chamber volume, mass burned percentage ranges from 6% to 17%, which suggests that the majority of ammonia is being burned inside the main chamber and only 6% to 17% of fuel mass is being burned in the sub-chamber. And it can be seen from the figure (about 11%, 6%, 7%, 9%, 17% at equivalence ratio 0.2, 0.4, 0.6, 0.8, and 1.0 respectivly) that under the conditions of an equivalence ratio of 0.4 and 0.6, the mixture burns the most in the main chamber, and the mixture burns the least in the main chamber under the condition of an equivalence ratio of 1.0. It shows that the combustion in the main combustor plays a decisive role in the final combustion pressure. That is, the more fuel burned in the main chamber, the better the overall combustion situation, which is reflected in more complete combustion, higher combustion pressure, and faster combustion speed.

4.2.4. Combustion duration

Figure 8 shows the combustion duration with different equivalence ratio at 298 K and **Table 3** compares the equivalence ratio 0.6 and 1.0 in **Figure 8**. From the total heat release calculated from the heat release rate curve, first 10% of heat release time is indicated as the blue line called the 0-10% combustion. Same as the blue line, orange line represents the main combustion of 10-90% combustion and gray line representing the last 10% of combustion. 0-10% combustion had the largest time increase as the equivalence ratio increases above and below 0.6. The largest difference in 0-10% was between equivalence ratio.
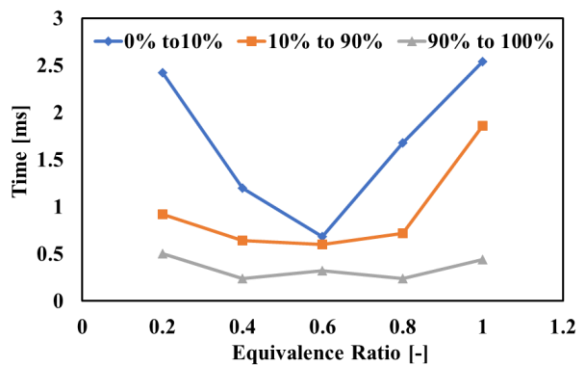

Figure 8. Specific combustion duration with different equivalence ratio at 298 K

0.6 and 1.0, where it had 1.86 ms of increase or 374% increase. The time increase in 0-10% combustion means that there was increase in ignition delay time.

Table 3. Comparison of combustion duration between ϕ 0.6 and ϕ1.2 at 298K

	$\emptyset 0.6$	$\emptyset 1.0$	delta
Total [ms]	1.60	4.84	3.24
0% ~ 10% [ms]	0.68	2.54	1.86
10% ~ 90 % [ms]	0.60	1.86	1.26
90% ~ 100% [ms]	0.32	0.44	0.12
O_2 [%]	41.8	25.4	-16.4

The 10-90% combustion had an increase in the duration above equivalence ratio 0.8, where it suggests the flame speed is slower at the stoichiometry. It has been reported that higher oxygen content in combustion results in higher flame temperature, thus it will have faster flame propagation speed [6]. Comparing the equivalence ratio 0.6 and 1.0, the oxygen content changes by nearly 16%. Oxygen content could have played large factor in the combustion duration. The 90-100% combustion duration was similar with all equivalence ratios.

4.2.5. Mean flame speed

Figure 9 shows the mean flame speed with the different equivalence ratios at 298K condition calculated using equation 5. The flame speed outputs the rough estimate of the flame propagation velocity during the entire combustion process including both aspects of laminar flame velocity and turbulent flame velocity. Equivalence ratio 0.6 was calculated to have the highest flame speed of 57.5 m/s due to the equivalence ratio 0.6 having the lowest total combustion period. Although the ammonia laminar burning velocity itself did not increase from the results of the observation of the combustion in the sub-chamber, the unburned mixture in the main combustion chamber was compressed by the burned gas in the sub-chamber to make it self-ignite and realized HCCI combustion. This combustion process greatly increased the combustion speed as a whole. The maximum laminar burning velocity of the ammonia and oxygen mixture is 1.1 m/s [25]. The mean flame speed obtained in this experiment is 52 times the laminar combustion velocity.
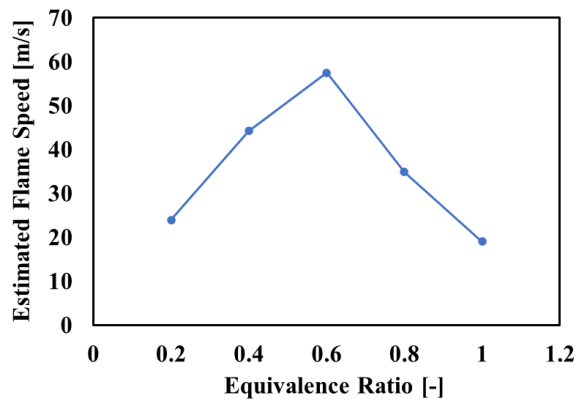
Figure 9. Mean flame speed with different equivalence ratio

5. Conclusion

The present study conducted the mixed combustion experiments of ammonia and oxygen in a constant volume combustor under the various equivalence ratio conditions. The important conclusions obtained from this study were summarized below.

1. Due to the existence of the sub-chamber, unburned gas was ejected from the sub-chamber by expanded burned gas, compressing the unburned gas in the main combustor., and then compressed and turbulent unburned gas in the main-chamber was rapidly burned as HCCI combustion. With this combustion method, the issue of the low laminar burning velocity of the ammonia has the posibility to solve.

2. With change in the equivalence ratio, highest in-cylinder pressure was measured with equivalence ratio 0.4, which is 2.5MPa (absolute pressure), and fastest combustion duration was measured at equivalence ratio 0.6, which is 57.5 m/s. This is because higher oxygen content in the lean condition is considered the reason for higher flame temperature and higher flame propagation velocity.

_____

Author's Declaration

Authors' contributions and responsibilities

The authors made substantial contributions to the conception and design of the study. The authors took responsibility for data analysis, interpretation and discussion of results. The authors read and approved the final manuscript.

Funding

Availability of data and materials

All data are available from the authors.

Competing interests

The authors declare no competing interest.

Additional information

No additional information from the authors.

_____

References

[1] J. Houghton, "Global Warming", *Reports on Progress in Physics*, vol. 68, no. 6, pp.1343-1403, 2005, doi: 10.1088/0034-4885/68/6/R02.

[2] Ministry of Land, Infrastructure, Transport and Tourism, Japan, retrieved from https://theicct.org/chart-library-passenger-vehicle-fuel-economy on 09 August 2021.

[3] W. Anggono, A. Hayakawa, E. C. Okafor, G. J. Gotama, and S. Wongso, "Laminar Burning Velocity and Markstein Length of CH4/CO2/Air Premixed Flames at Various Equivalence Ratios and CO2 Concentrations Under Elevated Pressure", *Combustion Science and Technology*, vol. 193, no. 14, pp. 2369–2388, 2021, doi: 10.1080/00102202.2020.1737032.

[4] A. C. Arifin, A. Aminudin, and R. M. Putra, "Diesel-biodiesel Blend on Engine Performance: An Experimental Study", *Automotive Experiences*, vol. 2, no. 3, pp. 91–96, 2019, doi: 10.31603/ae.v2i3.2995.

[5] E. Marlina, M. Basjir, M. Ichiyanagi, T. Suzuki, G. J. Gotama, and W. Anggono, "The Role of Eucalyptus Oil in Crude Palm Oil as Biodiesel Fuel", *Automotive Experiences*, vol. 3, no. 1, pp. 33–38, 2020, doi: 10.31603/ae.v3i1.3257.

[6] M. Wahyu, H. Rahmat, and G. J. Gotama, "Effect of Cassava Biogasoline on Fuel Consumption and CO Exhaust Emissions", *Automotive Experiences*, vol. 2, no. 3, pp. 97–103, 2019, doi: 10.31603/ae.v2i3.3004.

[7] M. Aziz, A. TriWijayanta, and A. B. D. Nandiyanto, "Ammonia as Effective Hydrogen Storage: A Review on Production, Storage and Utilization", *Energies*, vol. 13, no. 12, paper no. 3062, 2020, doi: 10.3390/en13123062.

[8] A. Hayakawa, T. Goto, R. Mimoto, Y. Arakawa, T. Kudo, and H. Kobayashi,

"Laminar Burning Velocity and Markstein Length of Ammonia/Air Premixed Flames at Various Pressures", *Fuel*, vol. 159, pp. 98–106, 2015, doi: 10.1016/j.fuel.2015.06.070.

[9] M. Koike, H. Miyagawa, T. Suzuoki, and K. Ogasawara, "Ammonia as a Hydrogen Energy Carrier and Its Application to Internal Combustion Engines", *Journal of the Combustion Society of Japan*, Vol. 58, No. 184, pp. 99-106, 2016, doi: 10.20619/jcombsj.58.184_99.

[10] Y. Ashida, K. Arashiba, K. Nakajima, and Y. Nishibayashi, "Molybdenum-catalysed Ammonia Production with Samarium Diiodide and Alcohols or Water", *Nature*, 568, pp. 536–540, 2019, doi: 10.1038/s41586-019-1134-2.

[11] T. Saika, M. Nakamura, T. Nohara, and S. Ishimatsu, "Study of Hydrogen Supply System with Ammonia Fuel", *JSME International Journal, Series B*, vol. 49, no. 1, pp. 78-83, 2006, doi: 10.1299/jsmeb.49.78.

[12] Y. Xia, K. Hadi, G. Hashimoto, N. Hashimoto, and O. Fujita, "Effect of Ammonia/Oxygen/Nitrogen Equivalence Ratio on Spherical Turbulent Flame Propagation of Pulverized Coal/Ammonia Co-combustion", *Proceedings of the Combustion Institute*, vol. 38, no. 3, pp. 4043–4052, 2021, doi: 10.1016/j.proci.2020.06.102.

[13] Y. Xia, K. Hadi, G. Hashimoto, N. Hashimoto, and O. Fujita, "Experimental Study of the Turbulent Flame Propagation Behavior of Pulverized Coal/Ammonia Co-combustion in an O2/N2 Atmosphere within a Fan-stirred Closed Vessel", *The Proceedings of the Thermal Engineering Conference 2020*, no. 0087, doi: 10.1299/jsmeted.2020.0087.

[14] H. Takeishi, J. Hayashi, S. Kono, W. Arita, K. Iino, and F. Akamatsu, "Characteristics of Ammonia/N$_2$/O$_2$ Laminar Flame in Oxygen-enriched Air Condition", *Transactions of the Japan Society of Mechanical Engineers, Series B*, vol. 81, no. 824, paper no. 14-00423, 2015, doi: 10.1299/transjsme.14-00423.

[15] S. Ito, M. Uchida, T. Suda, and T. Fujimori, "Demonstration Test of Ammonia/Natural Gas Co-firing Power Generation with 2 MW Class Gas Turbine", *Journal of the Combustion Society of Japan*, vol. 61, no. 198, pp. 289-292, 2019, doi: 10.20619/jcombsj.61.198_289.

[16] C. W. Gross, and S. C. Kong, "Performance Characteristics of a Compression-ignition Engine Using Direct-injection Ammonia–DME Mixtures", *Fuel*, vol. 103, pp. 1069–1079, 2013, doi: 10.1016/j.fuel.2012.08.026.

[17] S. Frigo, and R. Gentili, "Analysis of the Behaviour of a 4-stroke SI Engine Fuelled with Ammonia and Hydrogen", *International Journal of Hydrogen Energy*, vol. 38, no. 3, pp. 1607–1615, 2013, doi: 10.1016/j.ijhydene.2012.10.114.

[18] M. Pochet, I. Truedsson, F. Foucher, H. Jeanmart, and F. Contino, "Ammonia-hydrogen Blends in Homogeneous-charge Compression-ignition Engine", *SAE Technical Papers*, paper no. 2017-24-0087, 2017, doi: 10.4271/2017-24-0087.

[19] H. Nakano, S. Kobayashi, T. Sako, K. Nishimura, and T. Ishiyama, "Research on Effect of Sub-chamber in Natural Gas Lean-burn Engine -Thermal Efficiency Improvement of Natural Gas Engine-", *Transactions of Society of Automotive Engineers of Japan*, vol.47, no.4, pp. 843-848, 2016, doi: 10.11351/jsaeronbun.47.843.

[20] Y. Takashima, H. Tanaka, T. Sako, and M. Furutani, "Evaluation of Engine Performance by Changing Specification of Pre-chamber Spark Ignition Plug under Lean Burn Condition", *Transactions of Society of Automotive Engineers of Japan*, vol. 45, no. 2, pp. 221-227, 2014, doi: 10.11351/jsaeronbun.45.221.

[21] J. Taniguchi, K. Komiyama, H. Yamawaki, and M. Tamura, "Development of a Pre-chamber Spark Plug of Gas Engine for Heat Pump Air-conditioner", *Transactions of Society of Automotive Engineers of Japan*, vol. 48, no. 2, pp. 211-217, 2017, doi: 10.11351/jsaeronbun.48.211.

[22] H. Sasaki, K. Yamada, and S. Watanabe, "Homogenous Charge Compression Ignition Engine with a Pre-chamber (Fundamental Characteristics of the Combustion)", *Transactions of the Japan Society of Mechanical Engineers, Series B*, vol. 79, no. 800, pp. 638-648, 2013, doi: 10.1299/kikaib.79.636.

[23] K. Otomo, S. Horikoshi, A. Yagi, M. Kitamura, and H. Sasaki, "A Study on Multi-stage Combustion of Homogeneous Charge Compression Ignition Engine", presented at

ICATYE, March 6, 2019, doi: 10.1299/jsmekanto.2019.25.19D07.

[24] B. Mei, X. Zhang, S. Ma, M. Cui, H. Guo, Z. Cao, and Y. Li, "Experimental and Kinetic Modeling Investigation on the Laminar Flame Propagation of Ammonia under Oxygen Enrichment and Elevated Pressure Conditions", *Combustion and Flame,*, vol. 210,

pp. 236–246, 2019, doi: 10.1016/j.combustflame.2019.08.033.

[25] Q. Liu, X. Chen, J. Huang, Y. Shen, Y. Zhang, and Z. Liu, "The Characteristics of Flame Propagation in Ammonia/Oxygen Mixtures", *Journal of Hazardous Materials*, vol. 363, pp. 187-196, 2019, doi: 10.1016/j.jhazmat.2018.09.073.